Glycobiology vol. 2 no. 5 pp. 411–418, 1992

Structure elucidation of sulphated oligosaccharides from recombinant human tissue plasminogen activator expressed in mouse epithelial cells

Günter Pfeiffer[1], Stephan Stirm[1], Rudolf Geyer[1,4], Karl-Hermann Strube[2], Aldert A.Bergwerff[3], Johannis P.Kamerling[3] and Johannes F.G.Vliegenthart[3]

[1]Biochemisches Institut am Klinikum der Universität, Friedrichstrasse 24, D-6300 Giessen, FRG [2]BASF Aktiengesellschaft, Hauptlabor, D-6700 Ludwigshafen, FRG [3]Bijvoet Center, Department of Bio-Organic Chemistry, Utrecht University, PO Box 80075, NL-3508 TB Utrecht, The Netherlands

[4]To whom correspondence should be addressed at: Biochemisches Institut am Klinikum der Universität, Friedrichstrasse 24, D-6300 Giessen, FRG

Sulphated N-linked carbohydrate chains isolated from recombinant human tissue plasminogen activator expressed in mouse epithelial (C127) cells were analysed as oligosaccharide alditols by methylation analysis, liquid secondary ion mass spectrometry, and one- and two-dimensional ^{1}H-NMR spectroscopy. The results demonstrate that the major component has the following novel structure: NeuAcα2-6Galβ1-4GlcNAcβ1-2[NeuAcα2-3Galβ1-4GlcNAcβ1-4]-Manα1-3[NeuAcα2-3(SO_4-6)Galβ1-4GlcNAcβ1-2Manα1-6]-Manβ1-4GlcNAcβ1-4[Fucα1-6]GlcNAc-ol.

Key words: ^{1}H-NMR spectroscopy/mass spectrometry/murine (C127) cells/recombinant t-PA/sulphated oligosaccharides

Introduction

Human tissue plasminogen activator (t-PA) is a glycosylated serine protease which converts plasminogen into plasmin (Bachmann, 1987; Fears, 1989; Higgins and Bennett, 1990). In order to obtain large quantities of this enzyme for clinical use, recombinant t-PA (rt-PA) has been expressed in a number of heterologous cells, including mouse epithelial (C127) cells (Wei *et al.*, 1986; Reddy *et al.*, 1987; Hansen *et al.*, 1988; Hamaguchi *et al.*, 1989; Tsuji *et al.*, 1990). The glycosylation of t-PA has been shown to influence its antigenicity (Tsuji *et al.*, 1990), enzymatic activities (Hansen *et al.*, 1988; Parekh *et al.*, 1989; Wittwer *et al.*, 1989) and pharmacokinetics (Tanswell *et al.*, 1989; Smedsrød and Einarsson, 1990; Tanigawara *et al.*, 1990). Therefore, intended clinical trials of rt-PA require a detailed analysis of its carbohydrate chains.

In previous studies (Pfeiffer *et al.*, 1989), we have shown that human uterine rt-PA from C127 cells contains oligomannose, small amounts of hybrid, and sialylated *N*-acetyllactosamine type *N*-glycans. Part of the latter components was found to carry sulphate, which could be tentatively assigned to be attached to C-6 of β-galactosyl residues, simultaneously substituted by sialic acid at C-3. Since such a sulphated NeuAcα2-3Gal unit represents a novel structural element in glycoprotein-*N*-glycans, we have carried out a detailed analysis of these sulphated sugar chains. The corresponding non-sulphated oligosaccharide fraction was similarly analysed for comparison.

Results

Isolation of oligosaccharides

Radiolabelled *N*-acetyllactosaminic rt-PA oligosaccharide alditols were separated by anion-exchange HPLC (Figure 1). Fractions containing trisialylated (F/S3.1) and monosulphated, trisialylated (F/S4.2) triantennary carbohydrate chains were collected as indicated. Starting from 120 mg of purified rt-PA, ~780 and 160 nmol of F/S3.1 and F/S4.2 were obtained, respectively, as determined by monosaccharide analysis (Pfeiffer *et al.*, 1989). The distribution of radioactivity (not shown) indicated that the glycans in fractions F/S3.1 and F/S4.2 represented ~29.7 and 5.7 mol%, respectively, of the total *N*-acetyllactosaminic carbohydrate chains. Compared to the glycoprotein material analysed in our previous study (Pfeiffer *et al.*, 1989), these fractions occurred in smaller proportions in this rt-PA preparation, whereas the amount of monosialylated species was increased.

Methylation analysis

In agreement with previous data (Pfeiffer *et al.*, 1989), methylation analysis of F/S3.1 and F/S4.2 demonstrated the presence of fucosylated, triantennary oligosaccharide alditols. As a characteristic feature, sulphated F/S4.2 glycans contained one 3,6-disubstituted Gal residue. In contrast to our earlier investigation, both fractions were found to contain trace amounts (< 10% of total glycans) of trisialylated tetraantennary chains (data not shown).

Positive-ion LSIMS of permethylated fraction F/S3.1

Aliquots of permethylated fraction F/S3.1 were analysed by positive-ion liquid secondary ion mass spectrometry (LSIMS) (Figure 2). The spectrum reveals a pseudomolecular ion $[M+H]^+$ at *m/z* 3771, consistent with a molecular composition of $NeuAc_3Hex_6HexNAc_4dHexHexNAc$-ol (where dHex is deoxyhexose, Hex is hexose, HexNAc is *N*-acetylhexosamine and HexNAc-ol is *N*-acetylhexosaminitol). Further characteristic signals are found at *m/z* 344 ($NeuAc^+$ minus methanol), 376 ($NeuAc^+$), 793 ($NeuAcHexHexNAc^+$ minus methanol), 825 ($NeuAcHexHexNAc^+$) and 3304/450 (fission of the *N,N'*-diacetylchitobiitol unit). The small signals at *m/z* 668 ($HexHexHexNAc^+$) and 4424 ($[M+H]^+$) accord with the presence of traces of trisialylated tetraantennary carbohydrate chains carrying one additional α-galactosyl residue [see Pfeiffer *et al.* (1989) and ^{1}H-NMR data]. The corresponding positive-ion LSIMS analysis of permethylated fraction F/S4.2 yielded no detectable signals.

Negative-ion LSIMS of permethylated desialylated fraction F/S4.2 (F/S4.2)*

In order to assign sulphate groups to distinct galactose residues, sulphated glycans were permethylated before (F/S4.2) and after (F/S4.2*) desialylation, and analysed by negative-ion LSIMS.

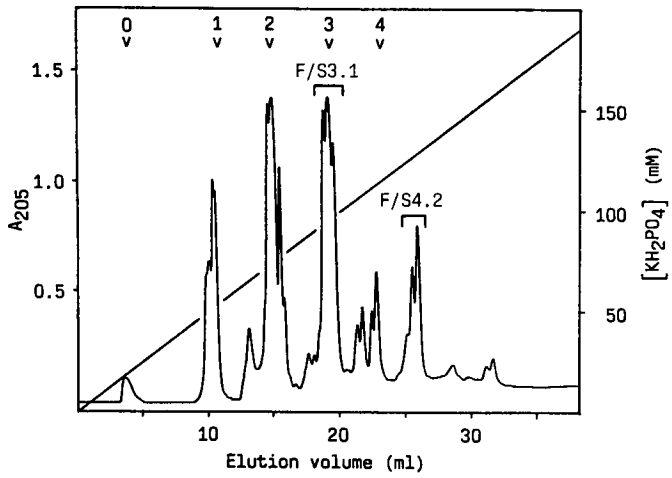

Fig. 1. Separation of charged *N*-acetyllactosamine type glycans from rt-PA by anion-exchange HPLC. Column, Mikropak-AX5, 4.6 × 250 mm; elution, linear gradient of potassium phosphate buffer (pH 4.4); flow rate, 1 ml/min. Numbers (0–4) with arrows, elution volumes of oligosaccharide standards with 0–4 sialic acid residues.

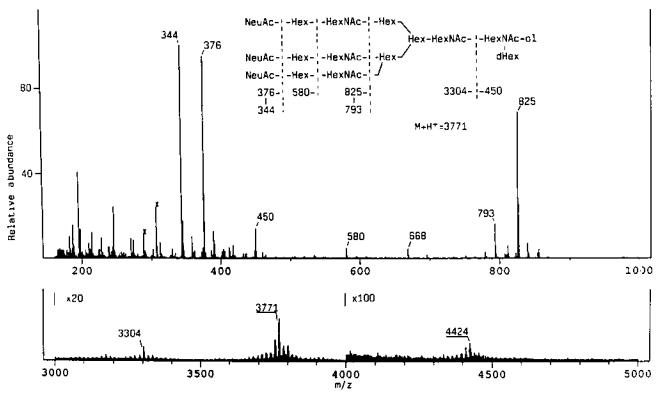

Fig. 2. Positive-ion LSIMS spectrum of methylated fraction F/S3.1. Pseudomolecular and characteristic fragment ions found are given in accurate masses rounded off to the next unit. Ions marked by 'X' arise from the matrix (3-nitrobenzyl alcohol) and unknown impurities commonly observed.

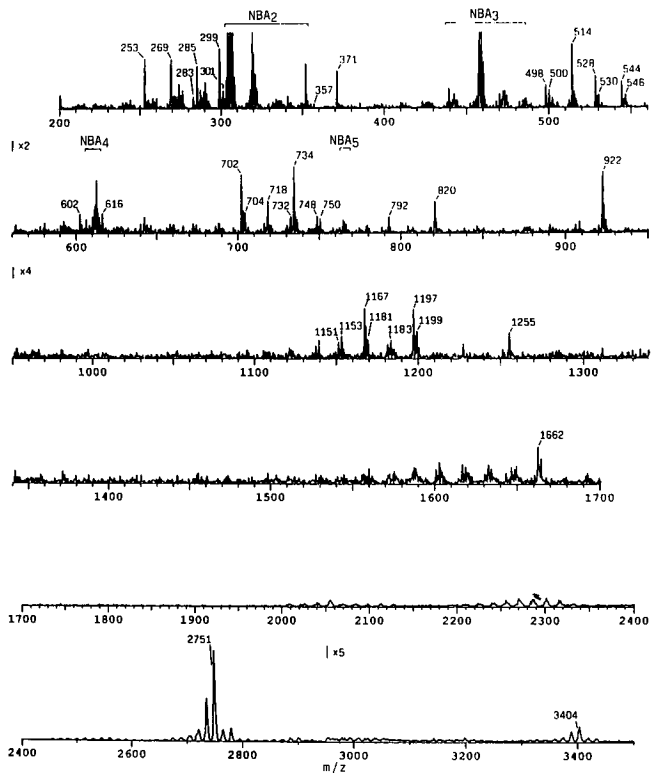

Fig. 3. Negative-ion LSIMS spectrum of methylated desialylated fraction F/S4.2 (F/S4.2*). Pseudomolecular and fragment ions are given in accurate masses rounded off to the next unit. Groups of signals designated 'NBA_{2-5}' represent mainly clusters of 3-nitrobenzyl alcohol, and/or small amounts of oxidation products thereof present as contaminants in the matrix.

The spectrum of the methylated asialo-oligosaccharide alditol fraction (Figure 3) contains a very intense pseudomolecular ion $[M-H]^-$ at *m/z* 2751, consistent with the molecular mass of monosulphated, monofucosylated, desialylated triantennary glycans. In addition, a weak signal is found at *m/z* 3404, which corresponds with the $[M-H]^-$ ion of a monosulphated, monofucosylated, desialylated tetraantennary chain carrying an additional hexose residue. The presence of small amounts of this type of component in F/S4.2* is supported by the methylation analysis data (see above) and the results obtained by ^{1}H-NMR spectroscopy (see below). The signals at $[M-H]^-$ -(n × 14) mass units are probably due to undermethylation.

The pattern of sulphated fragment ions closely resembles that reported for SO_4-GalNAc-containing glycans from ovine lutrophin (Dell *et al.*, 1991). Similar to these studies, the spectrum contains clusters of ions differing from each other by increments of sugar residues. The fragment ions at *m/z* 253, 269, 283, 285, 299 and 301 are derived from terminal SO_4-Gal, and can be explained by cleavage of the glycosidic linkage between Gal and GlcNAc and rearrangement of hydrogen atoms or loss of hydrogen atoms and/or methoxyl groups. The fragment ion at *m/z* 371 can be explained by ring cleavage of the adjacent GlcNAc, leaving C-4,5,6 still bound to the SO_4-Gal residue (Dell *et al.*, 1991).

Fragmentation of the linkage between GlcNAc and Man leads to an ion cluster ranging from *m/z* 498 to 546. Except for the peak at *m/z* 500, these signals appear 245 mass units higher than those of the cluster mentioned above, corresponding to a HexNAc increment. The fragment ions at *m/z* 602 and 616 can be explained by ring cleavage of the adjacent Man residue, yielding terminal elements containing Man C-2,3 (indicative of a 2-linked sulphated *N*-acetyllactosamine unit) and Man C-4,5,6 (indicative of a 4-linked sulphated *N*-acetyllactosamine element), respectively. This means that one part of the glycans carries sulphate at Gal-**8** (*m/z* 616), whereas in another part sulphate is linked to Gal-**6** or Gal-**6′** (*m/z* 602).

Signals of the cluster at *m/z* 702–750 are 204 mass units higher than those of the preceding cluster, reflecting a Hex increment. From the branching pattern of Man-**4** and Man-**4′**, as determined by methylation analysis (see above), it has to be concluded that this cluster is formed by cleavage of the linkage between Man-**4′** and Man-**3**. This assumption is further corroborated by the occurrence of signals at *m/z* 792 and 820, which can be explained by ring cleavage of Man-**3**, leading to terminal elements containing Man-**3** C-6,5, O-5 and C-6,5,4, respectively. Since the ion at *m/z* 792 can only be formed if the sulphated *N*-acetyllactosamine unit is linked to C-6 of Man-**3**, these results clearly indicate the presence of triantennary glycans carrying sulphate at Gal-**6′**.

The signal at *m/z* 922 can be assigned to the fragment SO_4-GalGlcNAcManMan formed by cleavage of the linkage

between Man-**3** and GlcNAc-**2**, and the combined loss of the substituent at C-3 of Man-**3**.

Fragmentation of the linkage between Man-**4** and Man-**3** leads to a cluster of ions at *m/z* 1151–1199. The relevant signals are 449 mass units higher (HexHexNAc increment) than those of the preceding cluster, indicating that these fragments comprise two *N*-acetyllactosamine elements, one of which is sulphated. The additional signal at *m/z* 1255 is obviously formed by ring cleavage of Man-**3**, yielding a fragment that contains Man-**3** C-3,2.

Except for the signal at *m/z* 1662, which may be produced from the pseudomolecular ion (*m/z* 2751) by ring cleavage of Man-**4** [fragmentation pathway D; see Dell, (1987)], the weak fragment ions in the higher mass region were not assigned.

Negative-ion LSIMS of permethylated sialylated fraction F/S4.2

Analysis of permethylated sialylated fraction F/S4.2 revealed pseudomolecular ions $[M-H]^-$ at *m/z* 3835 (major) and 4488 (minor), consistent with the molecular masses of monosulphated, monofucosylated, trisialylated tri- and tetraantennary glycans, respectively (Figure 4). The signal at *m/z* 269 is formed by cleavage of the linkage between Gal and GlcNAc, accompanied by loss of the sialic acid residue linked to C-3 of Gal. The clusters at *m/z* 614–732, 859–907 and 1063–1283 differ from the clusters at *m/z* 253–371, 498–546 and 702–922 of the desialylated sample (F/S4.2*) by 361 mass units (NeuAc increment), whereas the cluster at *m/z* 1873–1977 differs from the cluster at *m/z* 1151–1255 of F/S4.2* by 722 mass units (two NeuAc increments), thus verifying the structural assignments made above. The signal at *m/z* 818 is possibly formed by cleavage of the linkage between GlcNAc and Man, accompanied by loss of the (*N*-methyl)acetamido group (Dell *et al.*, 1991). The fragment ion at *m/z* 2023 corresponds to that at *m/z* 1662 in F/S4.2* (cf. Figure 3) and contains one sialic acid residue. In this case, however, unidentified fragment ions with *m/z* values <2023, which are found in low abundance in the corresponding region of the spectrum of the desialylated sample, partially overlap with the signals of the cluster at *m/z* 1873–1977.

Signals at *m/z* 963 and 977 (corresponding to those at *m/z* 602 and 616 in Figure 3) could only be detected by use of an array detector (see the insert in Figure 4). Since these ions are absent in the control spectrum taken prior to addition of the oligosaccharide sample (data not shown), their presence, however, is clearly significant and supports the conclusion drawn above that part of the glycans carry a sulphate group at Gal-**8**.

^{1}H-NMR analyses

The 500 MHz ^{1}H-NMR spectrum of fraction F/S3.1 (Figure 5A, Table I) indicates the presence of the following fucosylated, trisialylated triantennary carbohydrate chain as the major component.

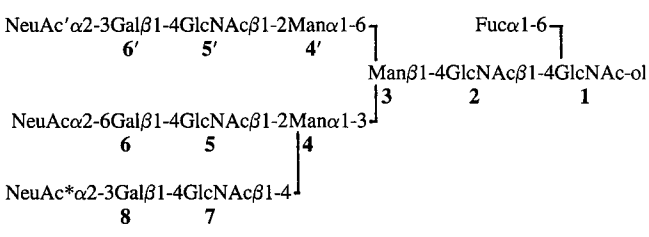

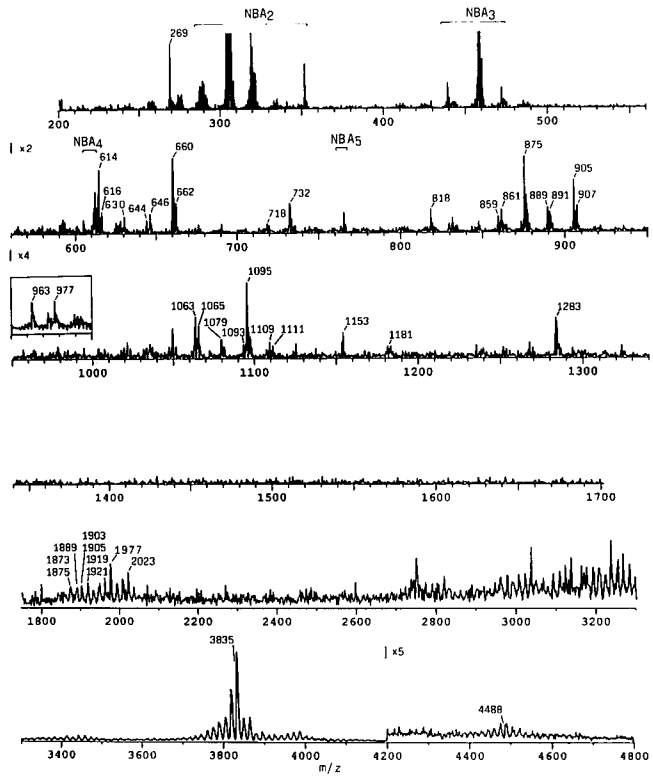

Fig. 4. Negative-ion LSIMS spectrum of methylated sialylated fraction F/S4.2. Designation of ions as in Figure 3.

The triantennary nature of the major component in fraction F/S3.1 is evident from the chemical-shift values of the Man H-1/H-2 signals (Vliegenthart *et al.*, 1983). The molar ratio of α2-3- and α2-6-linked NeuAc is roughly 2:1, as deduced from the intensities of the corresponding H-3e,3a signals. On guidance of the intensities of the Man-**4** and Man-**4'** H-1 resonances at δ 5.134 and δ 4.905, respectively, it can be concluded that for the major triantennary structure Gal-**6** (δ 4.443) bears a NeuAc in α2-6-linkage and Gal-**6'** a NeuAc in α2-3-linkage. The other α2-3-linked NeuAc residue resides on Gal-**8**, as supported by the GlcNAc-**7** NAc singlet at δ 2.076 (Van Pelt *et al.*, 1988). In fact, the structural reporter group signals of the peripheral elements match completely those of the non-fucosylated analogue (Green *et al.*, 1988; Krotkiewski *et al.*, 1990). Also, significant amounts of triantennary carbohydrate chains with NeuAcα2-6 at Gal-**6'** (Man-**4'** H-1, δ 4.932) and NeuAcα2-3 at Gal-**6** (Man-**4** H-1, δ 5.118) have to occur, whereas the absence of a GlcNAc-**7** NAc signal at δ 2.10 indicates that no α2-6-linked NeuAc is present at Gal-**8** (Van Pelt *et al.*, 1988). Because tri'-antennary oligosaccharides are absent (no Man-**3** H-2 signal at δ 4.26), the observation of the small signal at δ 4.870 (Man-**4'** H-1) indicates a low amount of tetraantennary structures (Van Pelt *et al.*, 1988). A small percentage of the components also have terminal α1-3-linked Gal (δ 5.148) (De Waard *et al.*, 1991).

The 500 MHz ^{1}H-NMR spectrum of fraction F/S4.2 (Figure 5B, Table I) demonstrates the occurrence of the following fucosylated, sulphated, trisialylated triantennary carbohydrate chain as the major component.

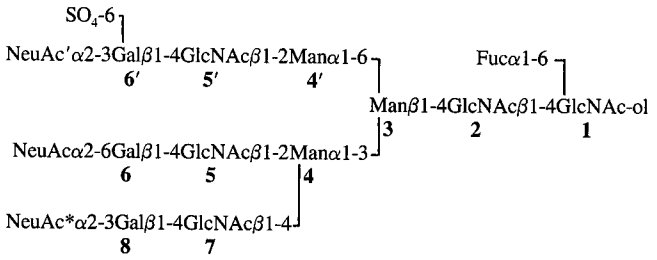

Although the ^{1}H-NMR spectrum of fraction F/S4.2 shows several similarities with that of fraction F/S3.1, including the presence of the triantennary components (Vliegenthart *et al.*, 1983), the sialylation pattern of the major triantennary component (Van Pelt *et al.*, 1988) and the α1-3-linked Gal (De Waard *et al.*, 1991), significant differences also exist, which have to be explained by the presence of glycan-bound sulphate. Comparison of the one-dimensional ^{1}H-NMR data of fractions F/S3.1 and F/S4.2 demonstrates typical shifts for Man-**4′** H-1 ($\Delta\delta$ +0.013) and H-2 ($\Delta\delta$ −0.005), suggesting that the sulphate group is part of the Manα1-6 branch. Furthermore, a number of additional changes are observed, namely a downfield shift of one of the three H-1 doublets at δ 4.547 to δ 4.582, a downfield shift of the Gal-**6′** (or Gal-**8**) H-3 signal from δ 4.117 to 4.138, and shifts of the H-3a,3e signals of one of the α2-3-linked NeuAc residues, whereas in the region δ 4.15–4.20 additional signals are detected. In order to obtain information about the specific location of the sulphate group

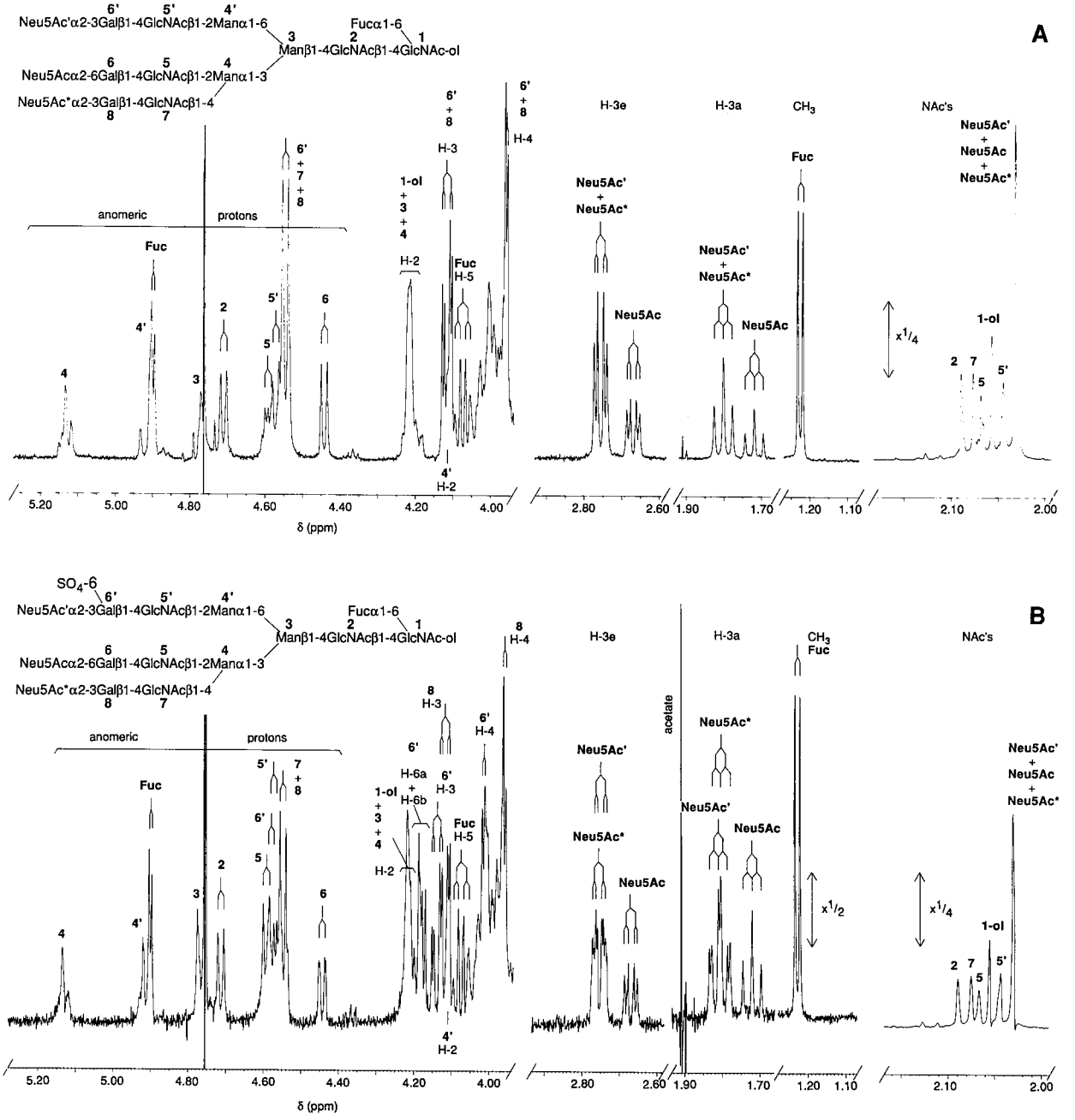

Fig. 5. Structural reporter group regions of the resolution-enhanced 500 MHz ^{1}H-NMR spectra of oligosaccharide alditols obtained from rt-PA. (**A**) Fraction F/S3.1; (**B**) fraction F/S4.2.

in the Manα1-6 branch, the two-dimensional homonuclear Hartmann–Hahn (HOHAHA) and rotating-frame nuclear Overhauser enhancement spectroscopy (ROESY) spectra of both fractions (Figure 6, F/S3.1; Figure 7, F/S4.2) were analysed. As compared to the HOHAHA spectrum of fraction F/S3.1, the HOHAHA spectrum of fraction F/S4.2 shows separate H-1 tracks for Gal-**6′** and Gal-**8**, providing the H-2,3,4 resonances for each residue. Correlating the intra-residual rotating-frame nuclear Overhauser enhancement (ROE) cross-peak on the Gal-**6′** H-1 track at δ 3.97 (Gal-**6′** H-1, Gal-**6′** H-5) in the ROESY spectrum of fraction F/S4.2 with the cross-peak at the same value (Gal-**6′** H-5) on the δ 4.18 track in the HOHAHA spectrum of the same fraction identifies the strong coupling pattern outside the bulk signal at δ 4.18 as belonging to Gal-**6′** H-6a,6b. It is clear that the presence of the sulphate group at C-6 gives rise to significant downfield shifts of Gal-**6′** H-6a,6b. A similar pattern of Gal H-6a,6b signals has been observed earlier in the case of $\Delta_{4,5}$GlcAβ1-3GalNAcβ1-4GlcAβ1-3Galβ1-3(SO_4-6)Galβ1-4Xylitol (De Waard *et al.*, 1992). A trace of a non-sulphated NeuAcα2-3Gal element in the Manα1-6 branch cannot be excluded (shoulder at δ 4.905), suggesting that components can also occur in small amounts, having the sulphated element on one of the other antennae.

Table I. ^{1}H-chemical shifts of structural reporter group protons of the constituent monosaccharides of the oligosaccharide alditols in fractions F/S3.1 and F/S4.2 derived from human rt-PA (C127 cells). Chemical shifts are given at 300 K and measured in ^2H_2O relative to internal acetone (δ 2.225). Values in parentheses correspond to minor components (see also the text)

Reporter group	Residue	Chemical shift in	
		F/S3.1	F/S4.2
H-1	GlcNAc-**2**	4.711	4.712
	Man-**3**	4.772	4.775
	Man-**4**	5.134 (5.118)	5.134 (5.120)
	Man-**4′**	4.905 (4.932)	4.918 (4.928)
	GlcNAc-**5**	4.592	4.591
	GlcNAc-**5′**	4.572 (4.600)	4.571 (4.600)
	Gal-**6**	4.443 (4.544)	4.444 (4.544)
	Gal-**6′**	4.547	4.582
	GlcNAc-**7**	4.547	4.547
	Gal-**8**	4.547	4.547
	Fucα1-6	4.900	4.900
	Galα1-3	(5.148)	(5.147)
H-2	GlcNAc-**1**-ol	4.22	4.22
	Man-**3**	4.218	4.213
	Man-**4**	4.218	4.217
	Man-**4′**	4.112	4.107
H-3	Gal-**6**	3.666	3.665
	Gal-**6′**	4.117	4.138
	Gal-**8**	4.117	4.117
H-4	Gal-**6**	3.924	3.926
	Gal-**6′**	3.960	4.015
	Gal-**8**	3.960	3.960
	Gal (Galα1-3)	(4.184)	(n.d.)
H-5	Gal-**6′**	n.d.	3.97
H-6a/6b	Gal-**6′**	n.d.	4.18
H-3a	NeuAcα2-6	1.720	1.720
	NeuAc′α2-3	1.803	1.810
	NeuAc*α2-3	1.803	1.803
H-3e	NeuAcα2-6	2.669	2.670
	NeuAc′α2-3	2.756	2.753
	NeuAc*α2-3	2.756	2.756
H-5	Fucα1-6	4.074	4.074
CH_3	Fucα1-6	1.226	1.226
NAc	GlcNAc-**1**-ol	2.056	2.056
	GlcNAc-**2**	2.089	2.090
	GlcNAc-**5**	2.066 (2.045)	2.067 (2.045)
	GlcNAc-**5′**	2.044 (2.065)	2.044
	GlcNAc-**7**	2.076	2.076
	NeuAc (3×)	2.031	2.031

n.d., not determined.

Discussion

N-Acetyllactosamine type glycans of rt-PA, expressed in C127 cells, were separated according to charge by anion-exchange HPLC. As revealed by the elution profile (Figure 1), the relevant fractions (F/S3.1 and F/S4.2) represented mixtures of (at least) three different components. Since attempts to subfractionate each of the fractions by high-pH anion-exchange chromatography failed (data not shown), they were directly subjected to carbohydrate structure analysis.

Analytical data revealed that fraction F/S3.1 represented a mixture of fucosylated, trisialylated triantennary glycans with a major component carrying α2-3-linked NeuAc at Gal-**6′**,-**8** and α2-6-linked NeuAc at Gal-**6** (Figure 5A), and minor components having α2-6-linked NeuAc at Gal-**6′** and α2-3-linked NeuAc at Gal-**6**,-**8**. In addition, small amounts of similarly fucosylated, trisialylated tetraantennary species containing an additional α-galactosyl residue occur. Fraction F/S4.2 comprised an analogous mixture of tri- and tetraantennary oligosaccharide alditols, but bearing one sulphate group, the major triantennary component of which carried the sulphate group at C-6 of Gal-**6′** in combination with an α2-3-linked NeuAc (Figure 5B).

Negative-ion LSIMS provided evidence for the presence of a triantennary structural isomer carrying sulphate at Gal-**8** instead of Gal-**6′**, demonstrating that sulphate groups can be assigned to distinct *N*-acetyllactosamine antennae by this technique, even if mixtures of oligosaccharides are employed. The intensities of fragment ions obtained by this type of study, however, might not reflect the actual relative proportions of the individual components. It is reasonable to assume that isomers carrying sulphate at Gal-**8** occurred in small amounts only and could, therefore, not be detected by ^{1}H-NMR spectroscopy.

The presence of isomers in which sulphate is linked to Gal-**6** could be neither unambiguously verified nor excluded. Linked-scan experiments carried out to answer this question failed, probably due to the low intensity of the corresponding mother ions.

So far, *N*-acetyllactosamine type *N*-glycans have been reported to carry sulphate groups at C-3 of Gal (Kamerling *et al.*, 1988; De Waard *et al.*, 1991), at C-6 of GlcNAc (Kamerling *et al.*, 1988; Roux *et al.*, 1988; De Waard *et al.*, 1991) or at C-4 of GalNAc residues (Baenziger and Green, 1988; Dell *et al.*, 1991). The NeuAcα2-3[SO_4-6]Gal-**6′** or -**8** unit found

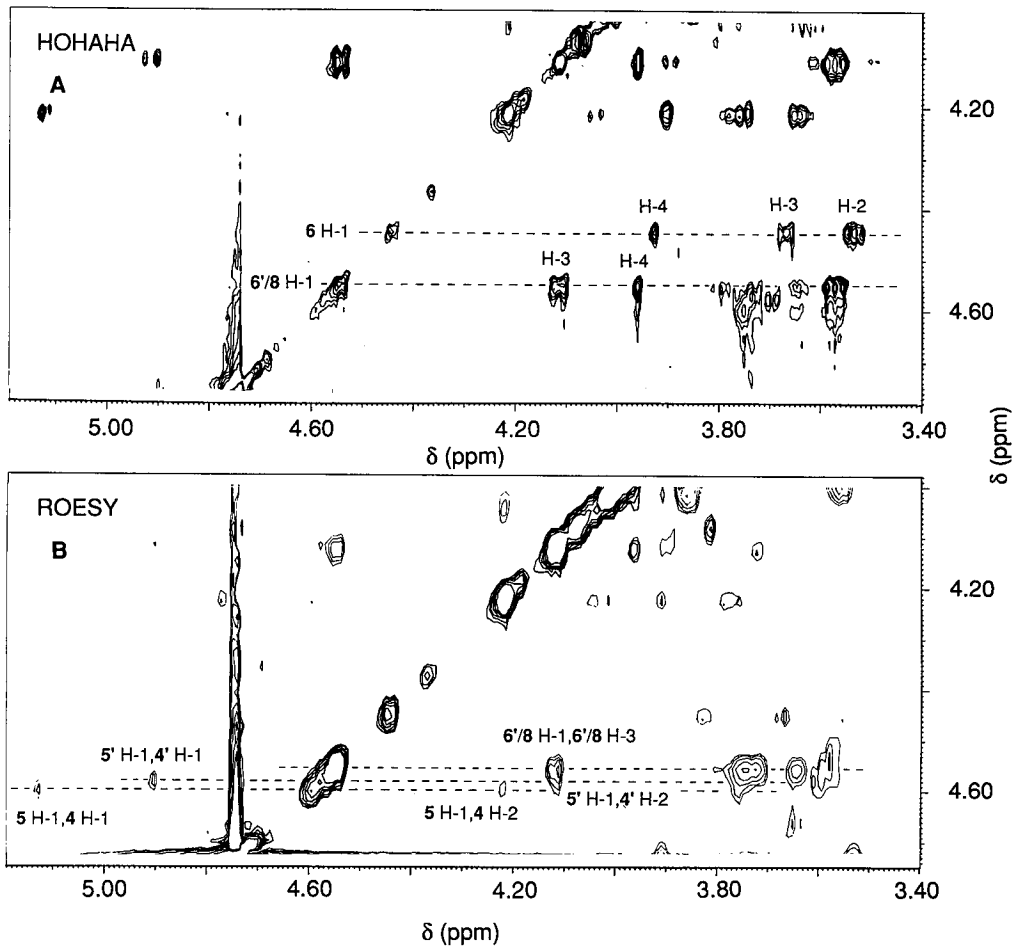

Fig. 6. Relevant parts of the 600 MHz two-dimensional HOHAHA (**A**) and two-dimensional ROESY (**B**) spectra of fraction F/S3.1. The bold numbers indicate monosaccharide residue numbers, as indicated in Figure 5 and the text. Correlations are presented by dashed lines.

in the sulphated triantennary glycans of rt-PA from C127 cells thus represents a novel structural element of glycoprotein-*N*-glycans. The question of whether this element might function as an antigenic determinant remains to be investigated. Furthermore, sulphation of rt-PA glycans might modulate the circulatory half-life of the glycoprotein, as reported recently for bovine lutrophin (Baenziger *et al.*, 1992).

Materials and methods

Preparation of rt-PA

Human uterine rt-PA was isolated from the culture supernatant of genetically manipulated C127 cells and purified as described by Pfeiffer *et al.* (1989), except that metabolic labelling was omitted.

Isolation of sulphated oligosaccharides

rt-PA (120 mg) was carboxymethylated and digested with trypsin (Serva, Heidelberg, FRG). Tryptic fragments were separated by reversed-phase HPLC (Pfeiffer *et al.*, 1989). N-Linked oligosaccharides were released from tryptic glycopeptide fractions I.1 and I.2 [see Figure 2 in Pfeiffer *et al.* (1989)] by treatment with peptide-N^4-(*N*-acetyl-β-glucosaminyl)asparagine amidase F from *Flavobacterium meningosepticum* (PNGase-F) (Boehringer, Mannheim, FRG), separated from residual peptides by reversed-phase HPLC, radiolabelled by reduction with NaB^3H_4, and desalted (Geyer *et al.*, 1983; Strube *et al.*, 1988). Oligosaccharide alditols were fractionated according to charge by anion-exchange HPLC on a Mikropak-AX5 column (Strube and Geyer, 1989) and monitored at 205 nm.

Methylation analysis

Oligosaccharide alditols were permethylated (Paz Parente *et al.*, 1985) and hydrolysed. Partially methylated alditol acetates, obtained after reduction and peracetylation, were analysed by capillary combined gas–liquid chromatography/mass spectrometry (GLC/MS) (Geyer *et al.*, 1983).

LSIMS

LSIMS analysis was carried out with a Finnigan MAT 900 (Finnigan MAT, Bremen, FRG) mass spectrometer, equipped with an array detector and a caesium gun which was operated at 23 kV with an emission current of 2–3 μA. Mass spectra of permethylated, non-sulphated glycans (~200 pmol) were recorded in the positive-ion mode at an accelerating potential of 5 kV with a magnet scan rate of 30 s/decade at a resolution of ~3000, and were acquired using a DEC 2100 data system. In the case of permethylated, sulphated oligosaccharide alditols, overlapping partial spectra were recorded in the negative-ion mode with a linear magnet scan (30 s/1000 mass units). Of each range, 4–8 single spectra were accumulated. Applying ~1 nmol of sample, no significant reduction of pseudomolecular ion intensity was observed within 40 min. Measurements using the array detector were carried out in the mass range *m/z* 950–1000 at constant magnetic field. In all experiments, 3-nitrobenzyl alcohol was used as matrix.

^{1}H-NMR spectroscopy

The oligosaccharide samples were repeatedly exchanged in 99.8% ^2H_2O (MSD isotopes) at p^{2}H 7 with intermediate lyophilization and finally dissolved in 99.96% ^2H_2O. Resolution-enhanced ^{1}H-NMR spectra were recorded on a Bruker AM-500 (Bijvoet Center, Department of NMR-spectroscopy, Utrecht University) or a Bruker AM-600 (NSR Center, University of Nijmegen, The Netherlands) spectrometer at 27°C. Chemical shifts are expressed in

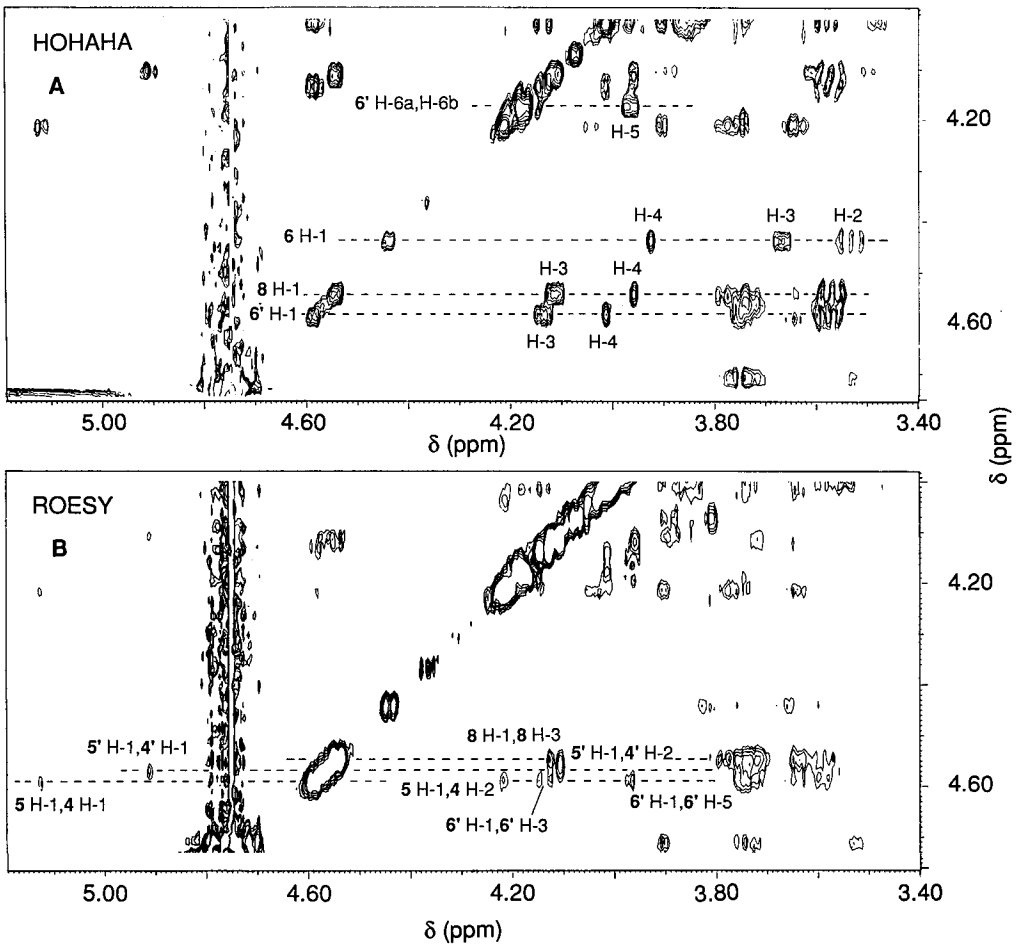

Fig. 7. Relevant parts of the 500 MHz two-dimensional HOHAHA (**A**) and two-dimensional ROESY (**B**) spectra of fraction F/S4.2. The bold numbers indicate monosaccharide residue numbers, as indicated in Figure 5 and the text. Correlations are presented by dashed lines.

p.p.m. by reference to internal acetone (δ 2.225 in ^2H_2O at 27°C) (Vliegenthart *et al.*, 1983).

The 600 and 500 MHz two-dimensional HOHAHA spectra of fractions F/S3.1 and F/S4.2, respectively, were recorded using the three-pulse sequence, 90°-t_1-MLEV-17-Acq (Bax and Davis, 1985; Marion *et al.*, 1989). A MLEV-17 mixing sequence of 120 ms was applied with a spin-lock field strength corresponding to a 90° ^{1}H pulse width of 23.3 and 27.1 μs for fractions F/S3.1 and F/S4.2, respectively. Data matrices of 512 × 2048 were recorded for both fractions (F/S3.1, spectral width of 3067 Hz in each dimension; F/S4.2, spectral width of 2100 Hz in each dimension).

The 600 and 500 MHz two-dimensional ROESY spectra of fractions F/S3.1 and F/S4.2, respectively, were obtained by a pulse scheme described as 90°-t_1- (spinlock)$_{\Phi+\pi/2}$-Acq(t_2) (Bothner-By *et al.*, 1984), with a spin-lock mixing pulse of 200 ms at a field strength corresponding to a 90° ^{1}H pulse width of 119 and 121 μs for fractions F/S3.1 and F/S4.2, respectively. Data matrices of 512 × 2048 were recorded for both fractions (F/S3.1, spectral width of 5000 Hz in each dimension; F/S4.2, spectral width of 2100 Hz in each dimension). The carrier frequency was placed at 5.7 p.p.m. for fraction F/S3.1 and on the 'water-line' at 4.8 p.p.m. for fraction F/S4.2.

In the case of the two-dimensional NMR experiments, the water signal was suppressed by presaturation. Phase-sensitive handling of data in the ω_1 dimension was carried out by the time-proportional phase increment method (Marion and Wüthrich, 1983). The time domain data of the HOHAHA and ROESY experiments were zero-filled to 1024 × 2048 data matrices prior to multiplication with a phase-shifted squared-bell and a phase-sensitive Fourier transformation.

Acknowledgements

We express our gratitude to Peter Kaese, Werner Mink and Siegfried Kühnhardt for methylation, GLC/MS and LSIMS analyses, to Pieter de Waard for introductory NMR analyses and to Hildegard Geyer for helpful discussions. This project was supported by the BASF Aktiengesellschaft (Ludwigshafen, FRG), the Deutsche Forschungsgemeinschaft (Sti 38/21-1 and Sonderforschungsbereich 272) and the Netherlands Foundation for Chemical Research (NWO/SON). The paper is in partial fulfilment of the requirements of G.P. for the degree of Dr.rer.nat. at Giessen University.

Abbreviations

dHex, deoxyhexose; GLC/MS, combined gas–liquid chromatography/mass spectrometry; GlcNAc-ol, *N*-acetylglucosaminitol; Hex, hexose; HexNAc, *N*-acetylhexosamine; HexNAc-ol, *N*-acetylhexosaminitol; ^{1}H-NMR, proton nuclear magnetic resonance; HOHAHA, homonuclear Hartmann–Hahn; LSIMS, liquid secondary ion mass spectrometry; MLEV, M. Levitt; PNGase-F, peptide-N^4-(*N*-acetyl-β-glucosaminyl)asparagine amidase F from *Flavobacterium meningosepticum*; ROE, rotating-frame nuclear Overhauser enhancement; ROESY, rotating-frame nuclear Overhauser enhancement spectroscopy; rt-PA, recombinant t-PA; t-PA, human tissue plasminogen activator.

References

Bachmann,F. (1987) Tissue plasminogen activator: chemical and physiological aspects. In Verstraete,M., Vermylen,J., Lijnen,H.R. and Arnout,J. (eds), *Thrombosis and Haemostasis*. International Society on Thrombosis and Haemostasis and Leuven University Press, Leuven, pp. 227–265.

Baenziger,J.U. and Green,E.D. (1988) Pituitary glycoprotein hormone oligosaccharides: structure, synthesis and function of the asparagine-linked oligosaccharides on lutropin, follitropin and thyrotropin. *Biochim. Biophys. Acta*, **947**, 287–306.